IOP Publishing Smart Materials and Structures
Smart Mater. Struct. **23** (2014) 065004 (10pp) doi:10.1088/0964-1726/23/6/065004

Development of self-healing polymers via amine–epoxy chemistry: II. Systematic evaluation of self-healing performance

He Zhang and Jinglei Yang

School of Mechanical and Aerospace Engineering, Nanyang Technological University, Singapore

E-mail: mjlyang@ntu.edu.sg

Received 23 December 2013, revised 5 February 2014
Accepted for publication 20 February 2014
Published 16 April 2014

Abstract

Part I of this study (H Zhang and J Yang 2014 *Smart Mater. Struct.* **23** 065003) reported the preparation and characterization of epoxy microcapsules (EP-capsules) and amine loaded hollow glass bubbles (AM-HGBs), and the modeling of a two-part self-healing system. In part II, the self-healing performance of this material system is systematically investigated. Various factors including the ratio, the total concentration and the size of the two carriers are studied as well as the healing temperature and the post heat treatment process. The best healing performance is obtained at a ratio of 1:3 of EP-capsules to AM-HGBs. It is observed that a higher concentration of larger carriers, together with a higher healing temperature, enables better healing behavior. Healing efficiency of up to 93% is obtained in these systems. In addition, post heat treatment decreases the healing efficiency due to stoichiometric mismatch of healing agents caused by leakage of amine in the HGBs at elevated temperature.

Keywords: self-healing polymer, fracture toughness, healing efficiency, thermal analysis, fractography

(Some figures may appear in colour only in the online journal)

1. Introduction

Successfully developed ways to realize homogeneous self-healing in epoxy include the embedding of hollow tubes [1–7], fabrication of microvascular networks [8, 9] incorporation of microcapsules [10–24], as well as molecular design using the reversible Diels–Alder reaction [25]. Depending on how many different parts of healing agents will be delivered to the crack plane, the specified methods can be divided into two groups, i.e. one-part self-healing systems and two-part self-healing systems. Systems in the first category include epoxy solution microcapsules [10, 11], single amine microcapsules [12], epoxy microcapsules/latent curing agent [13–16] and epoxy microcapsules/cationic catalyst [17–19], and systems in the second category include hollow tubes [1–6], microvascular networks [8, 9] and dual microcapsules [20–24].

For one-part self-healing epoxy systems, usually there is a second part which is incorporated into the matrix beforehand, such as the pre-dispersed Grubbs' catalyst for the dicyclopentadiene (DCPD)/catalyst system. The inclusive healing agent carriers can not only deliver healing agent to the damaged area, but also influence the original mechanical properties of the host matrix. Rule *et al* [26] established a quantitative relationship for the areal density of the delivered healing agent ($\bar{m}$) on the crack plane for one-part self-healing systems. It is found that $\bar{m}$ is proportional to the concentration and diameter of the incorporated capsules, which is verified by experiments [26, 27], as indicated by the healed peak load. However, the capsule inclusions will toughen the matrix but deteriorate other mechanical properties, like tensile strength, impact strength and flexural strength. Based on the selected mechanical parameter for the definition of self-healing efficiency, the nominal healing behavior can be influenced by both the released healing agent and the change of the original properties.

Two-part self-healing by epoxy chemistry based on dual healing agent carriers is more promising than the one-part

systems, in that the influence between the healing agents and the matrix is minimized by the protective shell of the carriers. Besides the areal density of the released healing agent, which is influenced by the incorporated concentration and size of the carriers, the stoichiometry of the two released parts is another paramount factor affecting the self-healing behavior. For two-part healing by hollow tubes or microvascular networks, in addition to the complexity of fabricating the hollow tubes or microvascular networks, it is hard to determine the stoichiometry of the two released healing agents, and consequently the healed mechanical properties. In the case of using encapsulated epoxy and polythiol by Yuan *et al* [21], it was found that the best healing behavior could be obtained when the ratio of the two capsules was kept at near 1:1. The highest healing efficiency of more than 100% could be achieved at room temperature (RT) when a total of 5 wt% capsules at a ratio of 1:1 were mixed into epoxy matrix. In the other case using encapsulated epoxy and amine by Jin *et al* [23], healing efficiency of about 91% could be gained at RT when the epoxy specimens were mixed with 17.5 wt% healing agent carriers in total with a ratio of 4:6 of amine microcapsule to epoxy microcapsule. However, in all of these two-part self-healing systems, no quantitative relationships were established to explain the healing trend when the parameters in the system varied.

In our previous investigations, we have reported the fabrication of epoxy microcapsules (EP-capsules) and amine loaded hollow glass bubbles (AM-HGBs), and their characterization in terms of their composition and thermal stability in the epoxy matrix [28, 29]. Two models were established for the two-part self-healing system in terms of the areal density, mass ratio and the longest diffusion distance of the released healants at the fracture plane. In this study, we continue the investigation to systematically evaluate the healing performance of the two-part self-healing system by the dual healing agent carriers by varying various parameters. The recovered mode-I fractured toughness using a short-grooved tapered double-cantilever beam (TDCB) specimen is adopted to assess the healing behavior.

2. Experiment

2.1. Materials

The Epolam 5015 and hardener 5015 used as the epoxy matrix were supplied by Axson. HGBs were ordered from 3M. All the chemicals, including diethylenetriamine (DETA) as curing agent for epoxy, 2,4,6-tris(dimethylaminomethylphenol) (DMP 30) as epoxy curing accelerator, ethyl phenyl acetate (EPA) as diluent for epoxy, were purchased from Sigma-Aldrich (Singapore) and used as received unless otherwise specified.

2.2. Preparation of self-healing specimens

The adopted EP-capsules and AM-HGBs were prepared and characterized in part I [29]. Two sizes of EP-capsules with diameters of 155.9 ± 23.7 μm and 255.7 ± 39.4 μm were used. 80 wt% Epolam 5015 in EPA was used as the core material for the EP-capsules. The measured content of epoxy monomer was 64 wt% for both sizes. Two sizes of AM-HGBs with diameters of 44.9 ± 6.2 μm and 66.9 ± 8.2 μm were applied. DETA with 10 wt% DMP 30 was used as the core material for the AM-HGBs. The measured content of DETA inside the etched HGBs was 30 wt% for both sizes.

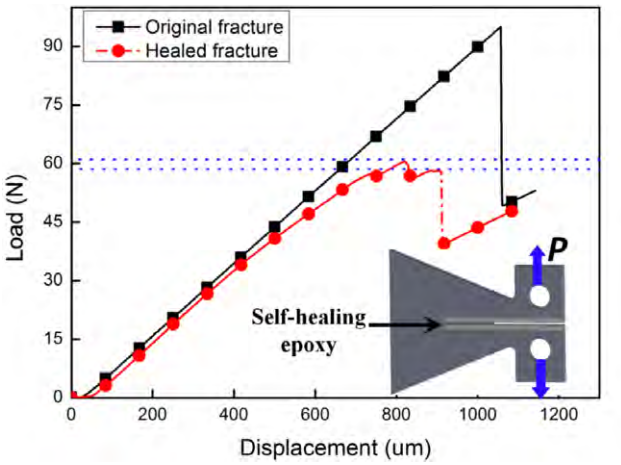

Figure 1. Typical load–displacement curves of the original fracture and healed fracture for the mode-I fracture toughness tests using a TDCB specimen as shown at the bottom right.

The healing behavior of this self-healing system was evaluated by the recovered mode-I fracture toughness using a TDCB specimen with a localized short groove [27], as shown at the bottom right in figure 1. The TDCB frames were fabricated using the neat epoxy resin, Epolam 5015, with its hardener 5015 at the ratio recommended, 100:30. Epoxy with dual healing agent carriers was poured into the short groove using the procedure as stated in our previous investigation [28]. The specimens were first cured at RT (~20 °C) for 24 h and then post-cured at 35 °C for another 24 h.

Self-healing epoxy specimens with various compositions were fabricated to explore the best self-healing performance, as shown in table 1. Under each specified condition, at least three specimens were manufactured to minimize the experimental error. Control specimens including samples made from pure epoxy and samples with only EP-capsules were also fabricated under the same conditions. The curing procedure for the control specimens was identical to that for the self-healing specimens. In order to study the effect of post-curing temperature on the healing performance, specimens with 10 wt% healing agent carriers at the optimized ratio of EP-capsule to AM-HGB were separately treated at 50 and 80 °C for 5, 10 and 16 h, as described in table 1.

2.3. Assessment of healing performance

Before testing, a pre-crack was induced by a sharp blade in each specimen. The fracture testing was carried out on an Instron machine (Instron Mini High Precision Tester) at a loading speed of 1 mm min^{-1} for the overhead. After fracture, the specimens were healed at RT, 35 °C and 50 °C for 24 h, respectively. Healing testing of the fracture toughness was conducted with the same parameters for comparison. Typical

Table 1. Specified parameters adopted in the experiment.

Adopted EP-capsule	Adopted HGB	Ratio of EP-capsule to AM-HGB	Total concentration (wt%)	Post heat treatment (h)
Big[a]	Big[b]	**1:1**	10.0	NA
Big	Big	**1:2**	10.0	NA
Big	Big	**1:2.5**	10.0	NA
Big	Big	**1:3**	10.0	NA
Big	Big	**1:3.5**	10.0	NA
Big	Big	**1:4**	10.0	NA
Big	Big	1:3	**5.0**	NA
Big	Big	1:3	**10.0**	NA
Big	Big	1:3	**12.5**	NA
Big	Big	1:3	**15.0**	NA
Big	Big	1:3	10.0	**T50-5**[c]
Big	Big	1:3	10.0	**T50-10**
Big	Big	1:3	10.0	**T50-16**
Big	Big	1:3	10.0	**T80-5**
Big	Big	1:3	10.0	**T80-10**
Big	Big	1:3	10.0	**T80-16**
Small[d]	**Big**	1:3	10.0	NA
Big	**Small**[e]	1:3	10.0	NA

[a] The diameter of the big microcapsule is 255.7 ± 39.4 μm.
[b] The diameter of the big HGB is 66.9 ± 8.2 μm.
[c] T50-5 means the samples are post treated at 50 °C for 5 h (similarly hereinafter).
[d] The diameter of the small microcapsule is 155.9 ± 23.7 μm.
[e] The diameter of the big HGB is 44.9 ± 6.2 μm.

load–displacement curves of a specimen for the original fracture and healed fracture are given in figure 1. The specimen was incorporated with 10 wt% healing agent carriers at a ratio of 1:3 for EP-capsules to AM-HGBs. The healing condition was 50 °C for 24 h. Using the TDCB geometry, the healing efficiency can be defined as [27]

$$\eta = \frac{K_{\mathrm{IC}}^{\mathrm{Healed}}}{K_{\mathrm{IC}}^{\mathrm{Original}}} = \frac{P_{\mathrm{C}}^{\mathrm{Healed}}}{P_{\mathrm{C}}^{\mathrm{Original}}} \tag{1}$$

where η is the healing efficiency, $K_{\mathrm{IC}}^{\mathrm{Healed}}$ and $K_{\mathrm{IC}}^{\mathrm{Original}}$ are the healed fracture toughness and the original fracture toughness, respectively, and $P_{\mathrm{C}}^{\mathrm{Healed}}$ and $P_{\mathrm{C}}^{\mathrm{Original}}$ are the healed peak load and original peak load separately.

In this investigation, as several peaks may appear on the load–displacement curve, the average of all the peaks was adopted for the calculation of healing efficiency:

$$\eta_{\mathrm{average}} = \frac{P_{\mathrm{Average}}^{\mathrm{Healed}}}{P_{\mathrm{Average}}^{\mathrm{Original}}}. \tag{2}$$

For the sample shown in figure 1, the original peak load is 95.1 N. As three peaks were given for the healing event, the average of the three peaks (59.2 N) was adopted as the healed peak load [23]. Consequently, the healing efficiency based on this definition is 62.3%.

For healing by manual injection, an excess amount of well-mixed epoxy with stoichiometric hardener was injected into the crack plane using a syringe. The injected specimens were cured at RT, 35 and 50 °C to check the best healing potential by the adopted epoxy–amine partners, and to observe the healing trend with regard to healing temperature.

2.4. Tensile properties of the formulated self-healing epoxy

The tensile properties of the self-healing epoxy were evaluated using dog-bone specimens according to ASTM standard D638. The formulated epoxy mixtures were added into rubber molds for molding, and then cured at RT for 24 h followed by 35 °C for another 24 h. The tests were carried out using an Instron machine (Instron 5500R) with a loading rate of 1 mm min^{-1}. The strain was recorded using an extensometer (Instron, Static Extensometer GL 25 mm) with gauge length of 25 mm.

In order to check the influence of the adhered amine solution from the AM-HGBs on the tensile properties, control specimens made from the matrix material (Epolam 5015 with hardener 5015 at 100:30) and extra amine solution (DETA with 10 wt% DMP 30) were fabricated. The added amounts were calculated based on the adhered percentage of amine outside the AM-HGBs according to the TGA curves as given in part I [29] for 5, 10 and 15 wt%. The curing and tensile testing procedure was the same as that for the self-healing epoxy specimens.

2.5. Other characterization methods

The fractography of the specimens was obtained using field emission scanning electronic microscopy (FESEM) (JEOL JSM-7600F), and the dispersion of the healing agent carriers in the matrix was characterized by optical microscopy (Olympus CKX41) in fluorescent mode.

3. Results and discussion

3.1. Healing behavior by manual injection of well-mixed epoxy–amine mixture

In order to obtain benchmark data for the adopted healing agents, the healing behavior by manual injection of epoxy resin well mixed with stoichiometric amine was studied at RT, 35 and 50 °C for 24 h. The injected mixture of epoxy (Epolam 5015) and amine hardener (DETA with 10 wt% DMP 30) was mixed at the stoichiometric ratio 100:15, according to their composition and functional groups. In order to fully wet the fractured surface for better healing behavior, an excess amount of the mixture was fed into the crack. The healing efficiency for this case with respect to the healing temperature is shown in figure 2. Healing efficiency as high as 75% was obtained at RT for 24 h. Although full healing ($\eta = 100\%$) was not achieved, an efficiency of about 90% was observed even at 35 °C. However, with further increase of the healing temperature, the improvement of the healing performance was marginal, which means that the relatively high healing temperature of 50 °C did not affect the healed fracture toughness. The enhancement of the fracture toughness by higher molecular weight and longer chains at higher temperature is offset by the embrittlement of the formed epoxy film with higher crosslinking density at higher temperature [30].

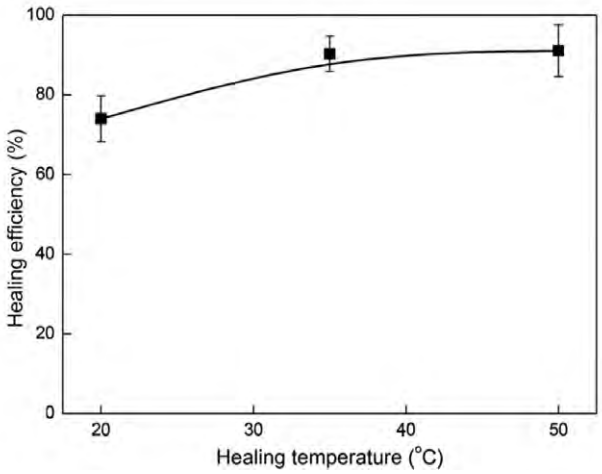

Figure 2. Healing efficiency of the control samples by manual injection of epoxy well mixed with stoichiometric hardener. The healing duration at each temperature is 24 h.

Table 2. Comparison of the healing by manual injection and by healing agent carriers in terms of original peak load, healed peak load and healing efficiency.

Parameters	Original peak load (N)	Healed peak load (N)	Healing efficiency (%)
Healing by injection	93.1 ± 7.7	84.8 ± 6.1	91.1 ± 6.5
Autonomous healing	105.5 ± 12.5	66.8 ± 13.9	63.3 ± 13.2

3.2. Optimization of mass ratio for EP-capsules to AM-HGBs

Given the significance of the stoichiometric match of the released healing agents for the two-part self-healing systems, the effect of the mass ratio of the incorporated EP-capsules to AM-HGBs on the healing behavior was studied when the total concentration of the healing agent carriers was held at 10 wt%. Figure 3 shows the change of healing efficiency, the original peak load, as well as the healed peak load, with respect to variation of the ratio of EP-capsules to AM-HGBs. The trend of the healing efficiency is consistent with that of the healed peak load when the ratio varies from 1:1 to 1:4. The best healing performance of about 64% was achieved when the ratio was 1:3 and the specimens were healed at 50 °C for 24 h. This healing efficiency is relatively low compared with that by injection of epoxy. Table 2 shows a comparison of the healing behaviors at 50 °C for 24 h by manual injection and healing agent carriers in terms of original peak load, healed peak load and healing efficiency. It is evident that the relatively low healing efficiency for autonomous healing results not only from the increase of the original fracture toughness but also from the lower healed fracture toughness. The difference between fully autonomous healing and healing by manual injection lies in three factors, i.e. the excess amount of the epoxy mixture, the optimized ratio for the two parts, and the better mixing.

Figure 4 shows the SEM images of the crack plane after the healing test. The imaged specimen was incorporated with 10 wt% healing agent carriers with a ratio of 1:3 of EP-capsules to AM-HGBs. Arrow 1 in figure 4(a) indicates the fractured

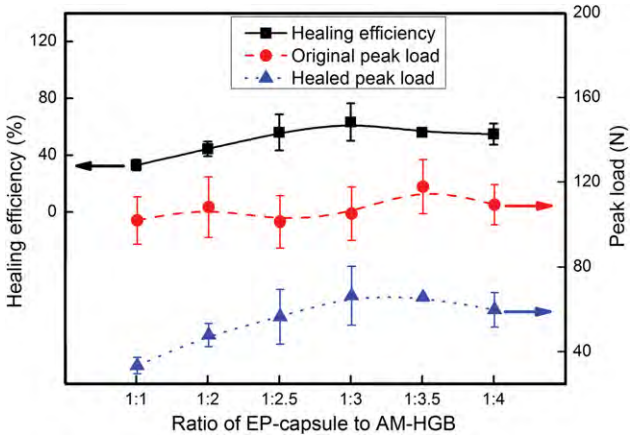

Figure 3. Healing efficiency, original fractured peak load and healed peak load with respect to mass ratio variation for microcapsules to HGBs at 50 °C.

AM-HGBs, and the enlarged image at the top right shows the cross-section of a fractured HGB. The shell of the HGB can be clearly seen from the inset. The frame in figure 4(a) indicating a fractured EP-capsule is enlarged in figure 4(b), and the inset at the top right shows the interface between the EP-capsule and the epoxy matrix. The fractured shell, as indicated by arrow 4, can be easily distinguished in the enlargement. The insets in figures 4(a) and (b) demonstrate that the two healing agent carriers, i.e. EP-capsules and AM-HGBs, are ruptured to release the healants upon the fracture event. The new epoxy formed by the released healing agents can be observed in figures 4(a) and (b), as indicated by arrow 3. This newly formed epoxy wedge at the fracture plane can adhere the two fractured faces of the specimen to bear some load after the healing process.

Evidently, this ratio for the two healing agent carriers seriously deviates from 100:13, which could be derived from the equivalent epoxide weight of the epoxy resin used and the theoretical functionality of the hardener (DETA, $n = 5$). Besides the incorporated concentration of the two healing agent carriers, the core percentage and the diameter of the healing agent carriers also make contributions to the final mass ratio of the released healants ($\overline{m_E}/\overline{m_A}$) at the fracture surface according to the model in part I [29] as

$$\frac{\overline{m_E}}{\overline{m_A}} = \frac{\overline{d_E}}{\overline{d_A}} \frac{\Phi_E}{\Phi_A} \frac{\omega_E}{\omega_A} \tag{3}$$

where $\overline{m_E}$ and $\overline{m_A}$ are the areal densities of the released epoxy and amine, $\overline{d_E}$ and $\overline{d_A}$ are the average diameters of the EP-capsules and AM-HGBs, Φ_E and Φ_A are the incorporated concentrations of the EP-capsules and AM-HGBs, ω_E and ω_A are the weight percentages of epoxy in the EP-capsules and DETA in the AM-HGBs. After substituting the specific values ($\overline{d_E} = 255.7 \pm 39.4\ \mu$m, $\overline{d_A} = 66.9 \pm 8.2\ \mu$m, $\Phi_E = 2.5$ wt%, $\Phi_A = 7.5$ wt%, $\omega_E = 64$ wt% and $\omega_A = 30$ wt%), a mass ratio of 2.73:1 for the released epoxy to released DETA can be obtained:

$$\frac{\overline{m_E}}{\overline{m_A}} = \frac{255.7\ \mu\text{m}}{66.9\ \mu\text{m}} \frac{2.5\ \text{wt\%}}{7.5\ \text{wt\%}} \frac{64\ \text{wt\%}}{30\ \text{wt\%}}. \tag{4}$$

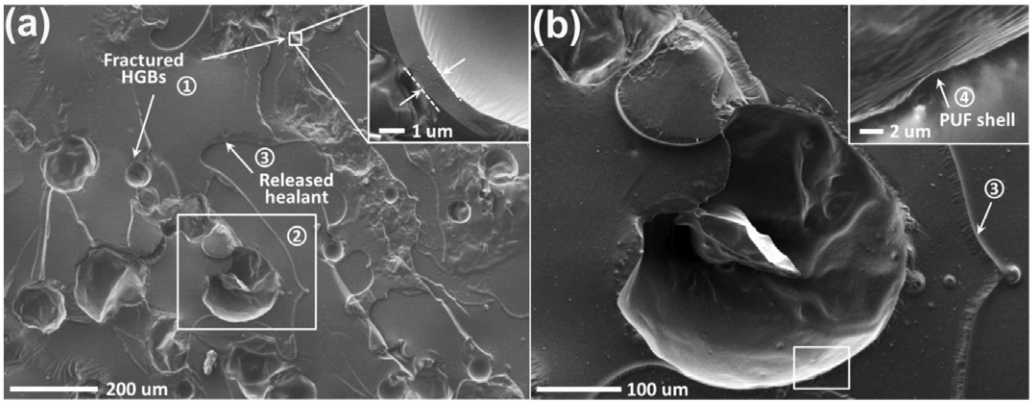

Figure 4. (a) SEM image of self-healing epoxy with 10 wt% carriers at the optimized ratio after the healing test; (b) enlargement of a fractured microcapsule and the epoxy healed by the released healant. The insets at the top right of (a) and (b) are the cross-sections of the fractured HGB and microcapsule, respectively.

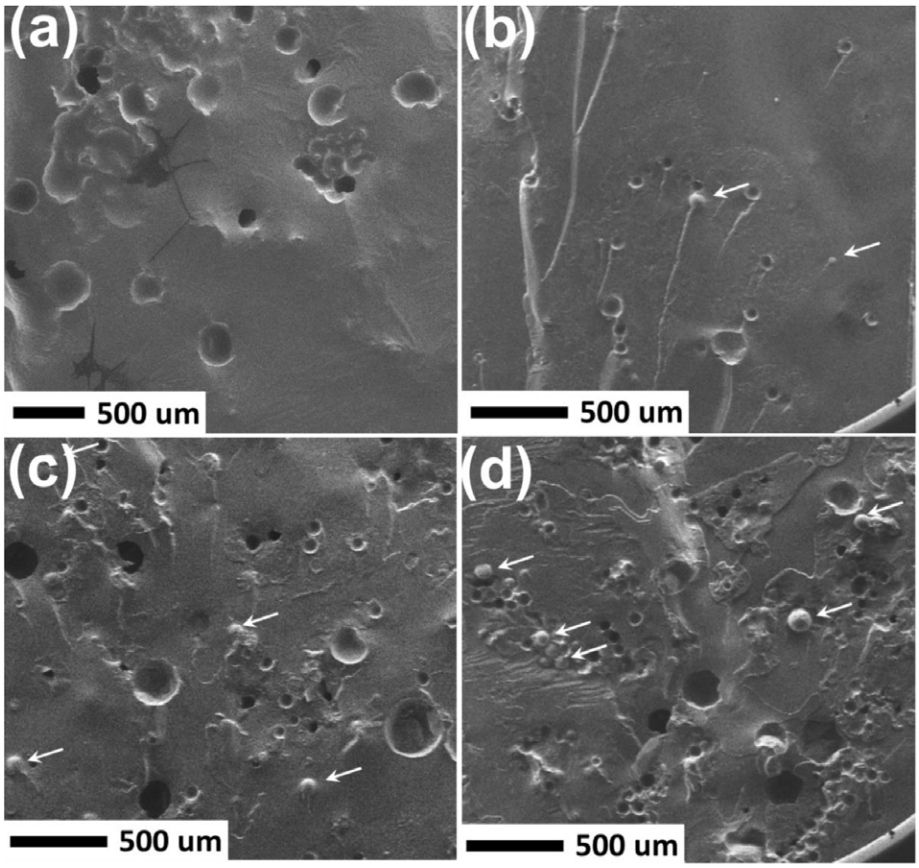

Figure 5. SEM images of the fracture surface for specimens with different concentrations at the optimized ratio: (a) control specimen with only EP-capsules; (b) 5 wt%; (c) 10 wt% and (d) 15 wt%. The arrows in the images indicate the unfractured HGBs at the fracture plane.

However, this ratio is still far different from the stoichiometric ratio, 100:13 (7.7:1), based on the epoxide group in Epolam 5015 and the reactive hydrogen atoms in DETA. Several reasons may account for the deviation. First of all, leakage of the loaded amine inside the shell through the holes during the manufacturing and curing stage is one of the most important factors. The optical image in figure 5 of part I [29] shows the epoxy thin film dispersed with 10 wt% EP-capsules and AM-HGBs at a ratio of 1:3 between two glass slides after the curing procedure at RT for 24 h ((a) and (b)) and then 35 °C for another 24 h ((c) and (d)). Although almost all the AM-HGBs are fully loaded with amine immediately after incorporation into an epoxy matrix, the appearance of fluorescent tails might mean that some of the amine solution diffuses out from the shell [29]. After the curing process, although only about 2% of the AM-HGBs are empty with no amine inside, about 15% of the AM-HGBs partially lose their loaded amine. Assuming that the partially loaded AM-HGBs after the curing process

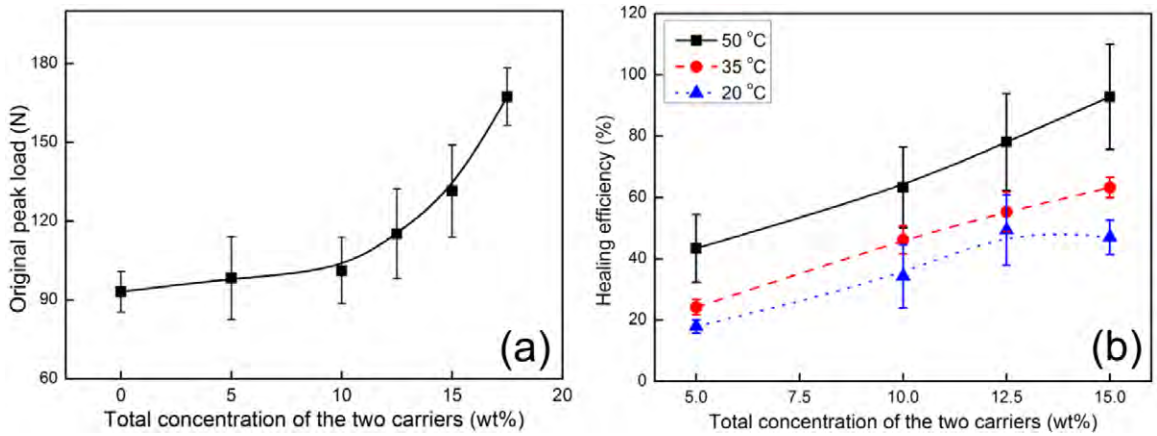

Figure 6. Influence of the incorporated carriers on (a) the original fracture toughness and (b) the healing behavior when the ratio of EP-capsules to AM-HGBs is fixed at 1:3.

can only deliver half of the original amount of carried amine solution, the modified ratio of core percentages (ω_E/ω_A) can be obtained as

$$\frac{\omega_E}{\omega_A} = \frac{64\ \text{wt\%}}{30\ \text{wt\%}\ (1 - 2\ \text{wt\%} - \frac{1}{2}15\ \text{wt\%})}. \quad (5)$$

Secondly, some of the AM-HGBs at the fracture surface were not ruptured by the crack tip during the fracture event while all the EP-capsules were ruptured, as shown in figures 5(b)–(d). This is slightly different from the assumption for the modeling that all the carriers intersected by the crack plane are ruptured to release healing agents. On one hand, the measured shell thickness of 0.79 μm with a large standard deviation 0.41 μm means that there are still some etched HGBs with relatively thicker shells which are strong enough to withstand the stress at the crack tip. On the other hand, the crack will bypass rather than go through the HGBs when the center of the HGB is too far away from the crack plane. When the approaching crack meets these two kinds of HGBs, interfacial debonding between the matrix and HGBs rather than rupture of the HGBs occurs, which does not trigger the release of the amine inside to take part in the healing reaction on the crack plane. By counting the numbers of ruptured and intact HGBs on the crack plane, about 15% of the total HGBs were not broken, as illustrated in figure 5. Assuming that all the unruptured HGBs did not deliver the carried amine solution to the crack plane, the modified ratio of concentrations (Φ_E/Φ_A) can be obtained as

$$\frac{\Phi_E}{\Phi_A} = \frac{2.5\ \text{wt\%}}{7.5\ \text{wt\%}\ (1 - 15\ \text{wt\%})}. \quad (6)$$

Taking these two factors into account, the mass ratio of the released epoxy to amine on the fracture plane is about 3.53:1, which is still a little far away from the stoichiometric ratio. Other factors that could also cause the deviation include the effective functionality of DETA when the specimens were healed at 50 °C and the influence of stoichiometry on the fracture toughness. The theoretical stoichiometric ratio is derived based on the assumption that the functionality of DETA equals 5. However, when the treating temperature is not high, the effective functionality of the hardener may not be able to reach its highest functionality, especially for a small molecule like DETA with high functionality. According to Selby and Miller [31], the highest fracture toughness of epoxy was achieved not at the stoichiometric ratio of epoxy to amine hardener, but at the point where moderate excess amine was given. The highest crosslinking density at the stoichiometric ratio does not benefit the fracture toughness.

3.3. Effect of total carrier concentration on healing performance

After optimization of the ratio of EP-capsules to AM-HGBs at 1:3, a set of experiments was conducted to study the influence of the total concentration of the two healing agent carriers on the healing behavior. First, the influence of the healing agent carriers on the original fracture toughness was investigated, as explained in figure 6(a). With increase of the concentration up to 10 wt%, the peak load increases gradually and steadily. However, after 10 wt%, the healing agent carriers affect the fracture toughness dramatically, leading to an exponential increase of the peak load. Factors responsible for this increase are the toughening effect of the healing agent carriers [23, 32] and the stoichiometric mismatch of the host matrix caused by the adhered amine outside the HGBs [31, 33–37]. Moreover, the higher the concentration of HGBs is, the more serious the mismatch is. Due to the increase of the original fracture toughness, the effect of the total concentration on the healing efficiency at higher concentration is seriously under-estimated.

The healing efficiency with regard to the total concentration is illustrated in figure 6(b). As can be seen from the graph, when healed at a higher temperature like 35 or 50 °C, the healing efficiency increases with increasing total carrier concentration. Average healing efficiency of about 93% was achieved when the concentration was increased to 15 wt%. The increase can be explained by the following two reasons. Firstly, with higher carrier concentration, more healing agents are

delivered to the fracture surface, according to the expression for $\bar{m}$ found in part I [29] as

$$\bar{m} = \rho_s d_c \Phi_c \omega_c. \quad (7)$$

This could be also verified by the SEM images of the fracture surface shown in figure 5 for concentrations of 5, 10 and 15 wt%. More surface areas, as well as the two carriers, were observed at higher concentration. Secondly, the two healing agents could be mixed better considering the two-part stoichiometric problem. As described by the cubic distribution model of the healing agent carriers in part I [29], the longest diffusion distance is inversely proportional to the cube root of the carrier concentration, which is applicable to both the EP-capsules and the AM-HGBs. With a shorter diffusion distance at higher concentration, better mixing and therefore better stoichiometry can be achieved, leading to improved healing performance.

However, when the system was healed at a lower temperature like RT, poor healing behavior was observed at higher concentration and the peak healing efficiency was found at a total concentration of 12.5 wt%. The trend before 12.5 wt% can be explained by the previously discussed reasons. For the trend after the peak, besides the discussed factors, the dramatic increase of the original peak load is responsible for the decrease of the healing efficiency. As determined by the definition of healing efficiency, the original fracture toughness has a huge effect on the final result. Although the absolute recovered fracture toughness increases, the relative increase compared to the original fracture toughness is poor, leading to the drop of the healing performance.

3.4. Size effect of the carriers on healing performance

In this study, two capsule sizes, i.e. 90–180 μm (155.9 $\pm$ 23.7 μm) and 180–300 μm (255.7 $\pm$ 39.4 μm), and two HGB sizes, i.e. 38–63 μm (44.9 $\pm$ 6.2 μm) and 63–90 μm (66.9 $\pm$ 8.2 μm), were adopted to compare the effect of carrier size on the healing behavior. The TGA curves, as given in part I [29], show that the neighboring sizes of the healing agent carriers have no obvious influence on the core content. From the obtained result shown in figure 7 for both EP-capsules and AM-HGBs, the larger the healing agent carriers, the better the healing performance. This finding is consistent with the observation [26] for one-part self-healing systems, because the areal density of healing agent delivered ($\bar{m}$) is positively proportional to the diameter of the healing agent carrier, according to equation (7). However, for this two-part system, besides the total amount of released healing agent, the stoichiometric mismatch of the two parts can also affect the healing behavior when varying the size of the carriers. For the EP-capsules, as the amount of epoxy released from the small microcapsules is less than that released from the large ones at the same concentration, the amount of amine released would exceed the required amount to obtain the highest fracture toughness. As illustrated in figure 7, the decrease of the healing efficiency for the smaller HGBs was more serious than the efficiency drop caused by the smaller microcapsules. For the AM-HGBs, the stoichiometric

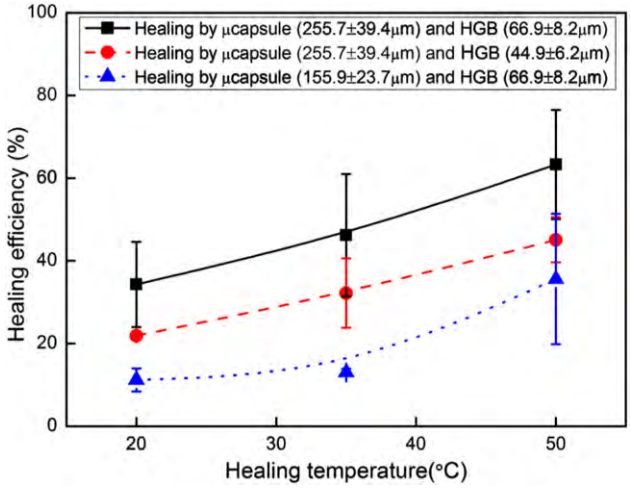

Figure 7. Influence of healing temperature and carrier size on the healing efficiency when 10 wt% carriers are incorporated at the optimized ratio.

mismatch due to the amount of healing agent released results from not only the above-mentioned reason, but also the much larger number of unbroken HGBs on the fracture surface. For hollow microspheres with similar shell thicknesses, a smaller one has a relatively higher crush strength [38]. Upon the fracture of the specimen, more small loaded HGBs were not ruptured compared to the large ones due to the relatively high crush strength, which can be seen from the SEM image of the fracture surface in figure 8. Attributed to this, the amount of amine released was much less than the required amount for the released epoxy on the fracture surface, leading to a more serious mismatch.

3.5. Effect of healing temperature on healing performance

The samples were healed at different temperatures to explore the effect of healing temperature on the healing efficiency, as shown in figure 7. Although the healing temperature does not have a large influence on the healing by manual injection especially after 35 °C, it is observed that the healing performance of the self-healing epoxy increases evenly from about 35% to 47%, and further to 64%, with increase of the healing temperature from RT to 35 °C, and finally to 50 °C, respectively. The healing temperature can influence the epoxy film formed in several ways. Higher temperature can speed up the reaction between the epoxy and the hardener on the fracture plane. Higher temperature also accelerates the evaporation of the solvent, EPA, and consequently decreases the time for the transformation from gel to solid polymer to bear more load. Finally, as well-mixed epoxy and amine can significantly increase the molecular weight and therefore give better mechanical properties, another large effect brought by the higher temperature is a fast diffusion rate for better mixing at the fracture surface.

3.6. Effect of post heat treatment of virgin samples on healing performance

The thermal stability of the loaded amine solution in the etched HGBs was investigated at both curing stages (RT for 24 h

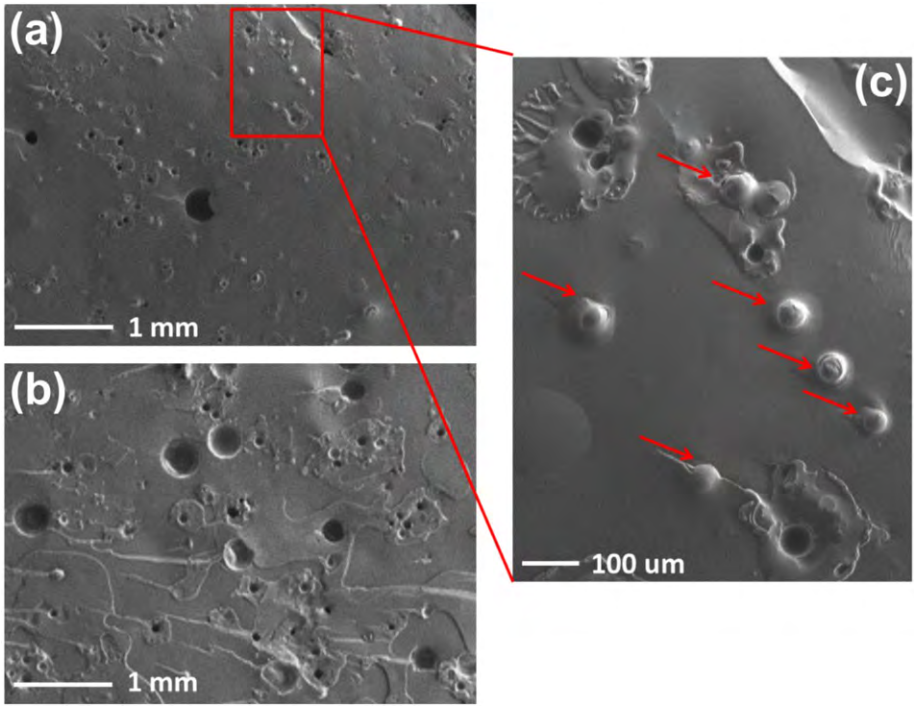

Figure 8. Unfractured HGBs on the fracture surface separately for a self-healing specimen with (a) small HGBs (44.9 ± 6.2 μm) and (b) large HGBs (66.9 ± 8.2 μm). (c) Enlargement taken from (a) to show the unfractured small HGBs.

and then 35 °C for another 24 h) and the post heat treatment stage (80 °C for different durations) when the AM-HGBs were mixed into the epoxy matrix [29]. Figure 9 shows the healing behavior of the specimens when they were healed at 50 °C for 24 h after being treated at 50 and 80 °C for 5, 10 and 16 h. A dramatic drop of the healing efficiency was observed at both treatment temperatures, especially for 80 °C. Compared with the huge drop of the healing performance at the early stage (the first 1 h) at 121 °C obtained by Jin *et al* [23], the healing performance falls roughly evenly during the investigated treatment duration, especially for 50 °C. Since epoxy is very stable before 200 °C, the diffusion of DETA from the etched HGBs through the holes at elevated temperature is responsible for this phenomenon, according to the TGA data shown in part I [29], and quantitative study of the thermal stability of the loaded amine solution. With the diffusion of the amine solution, the released epoxy and amine deviate from stoichiometry gradually, leading to a lower polymerization degree, and therefore lower mechanical properties and healing efficiency.

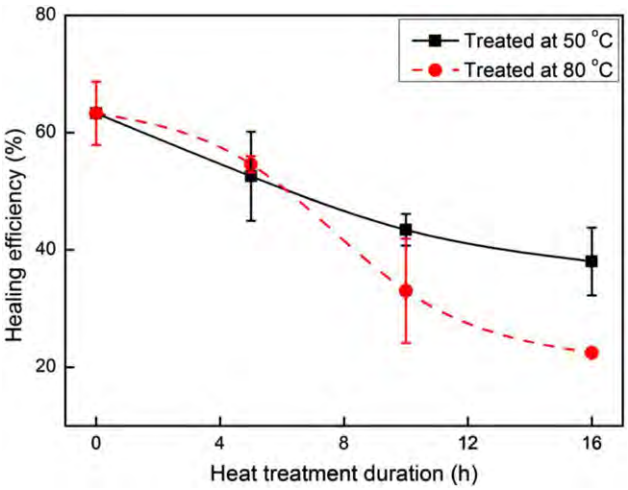

Figure 9. Influence of the post heat treatment at different temperatures on the healing performance when the specimens are mixed with 10 wt% carriers at the optimized ratio for the two parts, and healed at 50 °C for 24 h after fracture.

3.7. Influence of adding carriers on the tensile properties

As can be seen from figure 6(a), the fracture toughness was improved significantly by the incorporation of healing agent carriers due to the toughening effect of the inclusions and the lower crosslinking density because of the stoichiometric mismatch introduced by extra amine outside the HGB shell. However, those two effects will also deteriorate some other mechanical properties of the epoxy, like the tensile properties. Figure 10(a) shows typical stress–strain curves of pure epoxy and self-healing epoxy with 5, 10 and 15 wt% healing agent carriers at the optimized ratio. It is observed that the carrier inclusions are detrimental to the tensile properties. Figure 10(b) gives the trends of the tensile strength and elastic modulus with respect to the increase of the carrier concentration after the specimens were cured first at RT for 24 h followed by post-curing at 35 °C for another 24 h. While the modulus decreases from 2.67 to 2.14 GPa (80% of the original modulus), the strength decreases dramatically from 63.1 to 31.6 MPa (50%) from pure epoxy to epoxy with 15 wt% healing agent carriers. The influence of the adhered amine solution outside the AM-HGBs on the tensile properties

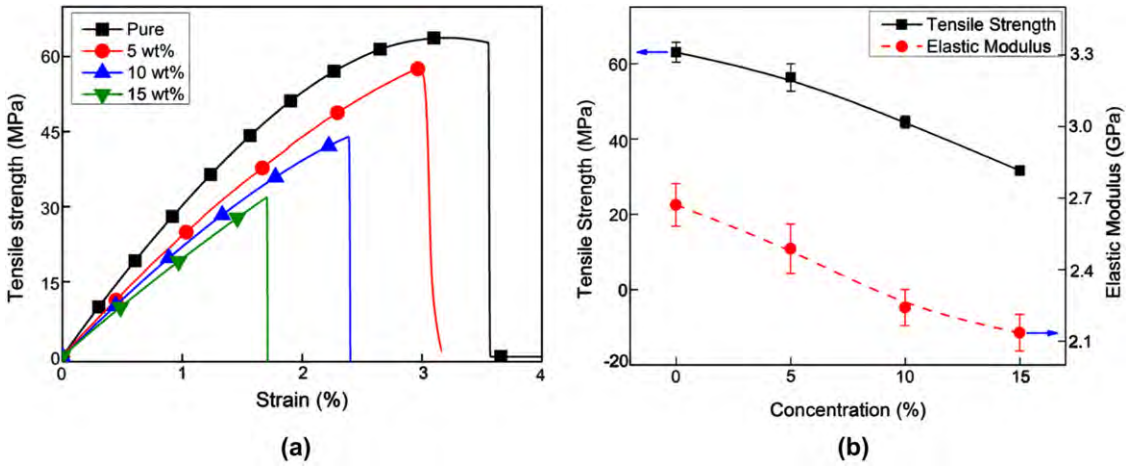

Figure 10. (a) Typical stress–strain curves for the pure epoxy and the self-healing epoxy with 5, 10 and 15 wt% carriers at the optimized ratio; (b) trend of tensile strength and modulus with respect to the total carrier concentration.

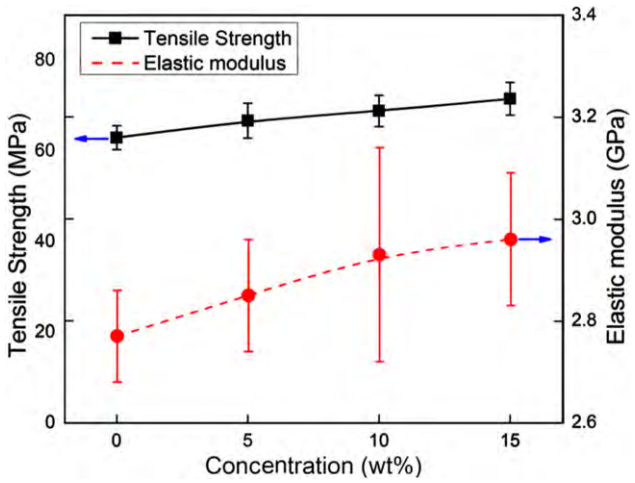

Figure 11. Influence of absorbed amine outside the AM-HGBs on the tensile properties of the epoxy matrix. The x-axis concentration means the incorporated concentration of healing agent carriers.

is shown in figure 11. It can be seen that both the tensile stress and the elastic modulus benefit a little from, or are at least insensitive to, the added extra amine solution. This result is consistent with the findings by other investigators when they studied the effect of non-stoichiometric curing on the tensile properties of epoxy [35]. As a result of this, the drop in the tensile properties of the self-healing epoxy can only be explained by the inclusion of the healing agent carriers. On one hand, EP-capsules with liquid inside can be treated as defective areas which cannot bear any load, especially for large microcapsules with polymeric shells [32]. Considering the large radius–thickness ratio, the AM-HGBs can also be treated like the microcapsules to some degree. On the other hand, although the inorganic HGBs can bear some load, the relatively weak bonding at the interface between the epoxy matrix and the shell will also compromise the properties upon tensile loading. The interfacial debonding between the HGBs and epoxy matrix can be clearly seen in figures 5(b), (c) and (d) for different concentrations of HGBs.

4. Conclusions

Systematic investigations were experimentally performed in this study to develop self-healing epoxy via two-part epoxy–amine chemistry carried by microcapsules and etched HGBs. Various factors were studied to explore their effects on the healing performance, and the healing model established in part I [29] was adopted to explain the healing behavior. The main conclusions can be summarized as follows.

(1) The ratio 1:3 for EP-capsules to AM-HGBs gives the best healing performance, although the mass ratio of the two released healants based on this ratio still deviates a long way away from the stoichiometry at free status.

(2) Better healing performance can be achieved when specimens with higher concentration of carriers with larger size are healed at higher temperature. The highest healing efficiency of about 93% is obtained when the self-healing epoxy is incorporated with 15 wt% large carriers (microcapsules of $255.7 \pm 39.4\ \mu$m and HGBs of $66.9 \pm 8.2\ \mu$m) under the optimized ratio and healed at 50 °C for 24 h.

(3) Thermal treatment of the self-healing samples at elevated temperature will accelerate the diffusion of amine from the etched HGBs, leading to stoichiometric mismatch of the released healants and therefore low healing efficiency.

(4) While the fracture toughness is improved by the incorporation of healing agent carriers, the tensile properties are seriously deteriorated in terms of the tensile strength due to the inclusions and the stoichiometric mismatch caused.

Acknowledgments

J Yang greatly acknowledges the financial support from NTU Start-up Grant and Singapore Ministry of Education Tier 1 research fund (Grant No. RG17/09).

References

[1] Motuku M, Vaidya U K and Janowski G M 1999 Parametric studies on self-repairing approaches for resin infused composites subjected to low velocity impact *Smart Mater. Struct.* **8** 623–38

[2] Bleay S M, Loader C B, Hawyes V J, Humberstone L and Curtis P T 2001 A smart repair system for polymer matrix composites *Composites* A **32** 1767–76

[3] Pang J W C and Bond I P 2005 A hollow fibre reinforced polymer composite encompassing self-healing and enhanced damage visibility *Compos. Sci. Technol.* **65** 1791–9

[4] Pang J W C and Bond I P 2005 'Bleeding composites'—damage detection and self-repair using a biomimetic approach *Composites* A **36** 183–8

[5] Williams G, Trask R and Bond I 2007 A self-healing carbon fibre reinforced polymer for aerospace applications *Composites* A **38** 1525–32

[6] Trask R S and Bond I P 2010 Bioinspired engineering study of Plantae vascules for self-healing composite structures *J. R. Soc. Interface* **7** 921–31

[7] Williams G J, Bond I P and Trask R S 2009 Compression after impact assessment of self-healing CFRP *Composites* A **40** 1399–406

[8] Toohey K S, Hansen C J, Lewis J A, White S R and Sottos N R 2009 Delivery of two-part self-healing chemistry via microvascular networks *Adv. Funct. Mater.* **19** 1399–405

[9] Hansen C J, Wu W, Toohey K S, Sottos N R, White S R and Lewis J A 2009 Self-healing materials with interpenetrating microvascular networks *Adv. Mater.* **21** 4143–7

[10] Caruso M M, Blaiszik B J, White S R, Sottos N R and Moore J S 2008 Full recovery of fracture toughness using a nontoxic solvent-based self-healing system *Adv. Funct. Mater.* **18** 1898–904

[11] Blaiszik B J, Caruso M M, McIlroy D A, Moore J S, White S R and Sottos N R 2009 Microcapsules filled with reactive solutions for self-healing materials *Polymer* **50** 990–7

[12] Li Q, Mishra A K, Kim N H, Kuila T, Lau K-t and Lee J H 2013 Effects of processing conditions of poly(methylmethacrylate) encapsulated liquid curing agent on the properties of self-healing composites *Composites* B **49** 6–15

[13] Yin T, Rong M Z, Zhang M Q and Yang G C 2007 Self-healing epoxy composites—preparation and effect of the healant consisting of microencapsulated epoxy and latent curing agent *Compos. Sci. Technol.* **67** 201–12

[14] Yin T, Zhou L, Rong M Z and Zhang M Q 2008 Self-healing woven glass fabric/epoxy composites with the healant consisting of micro-encapsulated epoxy and latent curing agent *Smart Mater. Struct.* **17** 015019

[15] Yin T, Rong M Z, Wu J, Chen H and Zhang M Q 2008 Healing of impact damage in woven glass fabric reinforced epoxy composites *Composites* A **39** 1479–87

[16] Yin T, Rong M Z, Zhang M Q and Zhao J Q 2009 Durability of self-healing woven glass fabric/epoxy composites *Smart Mater. Struct.* **18** 074001

[17] Xiao D S, Yuan Y C, Rong M Z and Zhang M Q 2009 Self-healing epoxy based on cationic chain polymerization *Polymer* **50** 2967–75

[18] Xiao D S, Yuan Y C, Rong M Z and Zhang M Q 2009 Hollow polymeric microcapsules: preparation, characterization and application in holding boron trifluoride diethyl etherate *Polymer* **50** 560–8

[19] Xiao D S, Yuan Y C, Rong M Z and Zhang M Q 2009 A facile strategy for preparing self-healing polymer composites by incorporation of cationic catalyst-loaded vegetable fibers *Adv. Funct. Mater.* **19** 2289–96

[20] Yuan Y C, Rong M Z, Zhang M Q, Chen B, Yang G C and Li X M 2008 Self-healing polymeric materials using epoxy/mercaptan as the healant *Macromolecules* **41** 5197–202

[21] Yuan Y C, Rong M Z and Zhang M Q 2008 Preparation and characterization of microencapsulated polythiol *Polymer* **49** 2531–41

[22] Yuan Y C *et al* 2011 Self-healing of low-velocity impact damage in glass fabric/epoxy composites using an epoxy-mercaptan healing agent *Smart Mater. Struct.* **20** 015024

[23] Jin H, Mangun C L, Stradley D S, Moore J S, Sottos N R and White S R 2012 Self-healing thermoset using encapsulated epoxy-amine healing chemistry *Polymer* **53** 581–7

[24] Jin H, Mangun C L, Griffin A S, Moore J S, Sottos N R and White S R 2014 Thermally stable autonomic healing in epoxy using a dual-microcapsule system *Adv. Mater.* **26** 282–7

[25] Tian Q, Yuan Y C, Rong M Z and Zhang M Q 2009 A thermally remendable epoxy resin *J. Mater. Chem.* **19** 1289–96

[26] Rule J D, Sottos N R and White S R 2007 Effect of microcapsule size on the performance of self-healing polymers *Polymer* **48** 3520–9

[27] Brown E N, Sottos N R and White S R 2002 Fracture testing of a self-healing polymer composite *Exp. Mech.* **42** 372–9

[28] Zhang H and Yang J 2013 Etched glass bubbles as robust micro-containers for self-healing materials *J. Mater. Chem.* A **41** 12715–20

[29] Zhang H and Yang J 2014 Development of self-healing polymers via amine-epoxy chemistry part I: properties of healing agent carriers and modelling of two-part self-healing system *Smart Mater. Struct.* **23** 065003

[30] Plangsangmas L, Mecholsky J J and Brennan A B 1999 Determination of fracture toughness of epoxy using fractography *J. Appl. Polym. Sci.* **72** 257–68

[31] Selby K and Miller L E 1975 Fracture toughness and mechanical behaviour of an epoxy resin *J. Mater. Sci.* **10** 12–24

[32] Brown E N, White S R and Sottos N R 2004 Microcapsule induced toughening in a self-healing polymer composite *J. Mater. Sci.* **39** 1703–10

[33] D'Almeida J R M and Monteiro S N 1996 Analysis of the fracture surface morphology of an epoxy system as a function of the resin/hardener ratio *J. Mater. Sci. Lett.* **15** 955–8

[34] Gupta V B, Drzal L T, Lee C Y C and Rich M J 1985 The temperature-dependence of some mechanical-properties of a cured epoxy-resin system *Polym. Eng. Sci.* **25** 812–23

[35] Kim S L, Skibo M D, Manson J A, Hertzberg R W and Janiszewski J 1978 Tensile, impact and fatigue behavior of an amine-cured epoxy-resin *Polym. Eng. Sci.* **18** 1093–100

[36] Mostovoy S and Ripling E J 1966 Fracture toughness of an epoxy system *J. Appl. Polym. Sci.* **10** 1351–71

[37] Robinson E J, Douglas E P and Mecholsky J J 2002 The effect of stoichiometry on the fracture toughness of a liquid crystalline epoxy *Polym. Eng. Sci.* **42** 269–79

[38] Keller M W and Sottos N R 2006 Mechanical properties of microcapsules used in a self-healing polymer *Exp. Mech.* **46** 725–33